한국도로포장공학회지
第2券 1號 2000年 3月
pp. 147 ~ 156

다짐밀도의 이론적 전개

Theoretical Development of Compaction Density

허 정 도* · 김 한 용** · 남 영 국***
Huh, Jung-Do · Kim, Han-Yong · Nam, Young-Kug

ABSTRACT

Compaction is known to critically affect pavement performance. Due to its importance, a theoretical modelling of compacted density in the term of number of roller coverages is attempted by assuming compaction process essentially identical to pavement rutting. Excellent data fittings by the developed equation may prove the validation of assumptions made as well as justification of its use. According to the derived equation, a plot of density difference with respect to number of roller coverages in the logarithmic scale produces a linear relationship. However, this linearity is turned out to be deviated by cooling effect, change of amplitude and frequency. Investigation of these three factors proposes a new generalized compaction density equation, which shows a promising future. By applying this general formula, the equations for the number of roller coverages required and the final compaction density obtained for a particular compaction project is derived first time in compaction research.

Key Words : Compaction Density, Mix Viscosity, Mix Temperature, Roller Coverage, Amplitude and Frequency of a Vibratory Roller, etc.

요 지

다짐은 포장 공용성에 중요한 영향을 미친다고 알려져 있다. 따라서 이 다짐공정을 포장의 소성변형과 근본적으로 동일하다고 가정하여, 다짐밀도를 롤러다짐수의 항으로 표현하는 이론 모델링식을 정립하였다. 정립된 식의 우수한 데이터 예측능력은 유도과정에 세운 가정들의 검증과 더불어 이 식의 사용 정당화에 대해 확신시켜준다. 유도된 식에 의하면, 대수밀도 차를 대수 다짐회수의 항으로 그림을 그리면 일차함수의 직선관계식이 주어진다. 그러나 이 직선관계는 공기온도에 의한 냉각과 진동롤러의 진폭과 주기 등의 효과가 존재하면 더 이상 성립되지 않음이 판명된다. 본 연구에서는 이러한 세 요인들에 대한 영향도 함께 연구하여 더 전반적이고 성공가능성을 보여주는 새로운 다짐밀도 식을 제안하였다. 이 제안식을 응용하여 특정다짐공정에 요하는 전체 롤러다짐회수와 최종다짐밀도를 구하는 관계식을 다짐연구 중 최초로 제시하였다.

핵심용어 : 다짐밀도, 혼합물점도, 혼합물온도, 롤러다짐회수, 진동롤러의 진폭과 주기, 등등.

* 인천대학교 토목공학과 방문교수
** 한솔 엔지니어링 사장
*** 인천대학교 토목공학과 교수

1. INTRODUCTION

A proper design of mix materials, homogeneity in asphalt mix, and an effective compaction may be the three most important factors governing quality of asphalt pavement surface layer. Among them, compaction is the most critical construction step on which pavement performance (i.e., rutting, fatigue cracking, various other cracks, etc.) heavily depends. In other words, compaction process builds the pavement internal structure to resist any external stress or loading applied.

As means of compaction, rolling equipments are used and commonly classified as two categories. One is static rollers (a 3-axle steel roller, a rubber tire roller, a pneumatic roller, and a tandem roller) and the other is vibratory rollers (a single or a double drum roller, and tandem rollers). Drum diameter, width and weight are characteristics of static rollers with operation variables such as number of roller coverages, roller speed, and compaction temperature, while vibratory rollers possess two additional variables, frequency and amplitude, in addition to those of static ones. Much effort was devoted in the past to find the effective compaction roller (a certain roller or a train of rollers) to achieve a high degree of compaction without any damage like pushing, shoving, checking, bleeding, hair-line cracks, etc. (Cechetini (1974) and Linden and Heide (1987)).

The best pavement performance is initially set by the hot mix design, but the design goal may fail or enhance according to compaction process. This is why compaction is the key step, and requires a careful control. In spite of importance, the qualitative experiments in the past restricted further improvement due to lack of scientific theories. For this reason, new compaction equations are proposed in this study. They could be useful tools in analysing compaction data, finding an effective roller (or a train of rollers), and modifying hot mix design to improve compaction performance, etc.

2. THEORY FOR A COMPACTION DENSITY EQUATION

Compaction density is the most popular description of compaction process. It is viewed as one-dimensional vertical compression starting from the top surface of lay-down mixes after completion of paver operation. By considering a control volume (V) having a mass (m) with a fixed cross-section (A) and a lift height (hd), a compaction density (ρ) can be defined as

$$\rho = \frac{m}{V} = \frac{m}{A\,h_d} \tag{1}$$

In compression, the compaction depth (h) from the initial top surface increases with density (ρ) growth, while the lift height (hd) counting from the bottom base decreases. In other words, the compaction depth (h) has an inverse relationship to the lift height; that is,

$$c\,(h - h_o) = \frac{1}{h_d} - \frac{1}{h_{do}} \tag{2}$$

where c, ho and hdo are a constant, an initial compaction depth (which is equal to zero) and an initial lift height.

Consideration of Eqs. 1 and 2 yields the following equation for compaction density change;

$$\rho - \rho_o = \frac{m}{A}\left\{\frac{1}{h_d} - \frac{1}{h_{do}}\right\} = \frac{cm}{A}h \tag{3}$$

Assume that the deformation mechanism of compaction process is essentially identical to rutting in permanent deformation, because both

are caused by the cyclic loading on pavement. For example, the initial rapid rut depth shown in the most of wheel tracking experiments usually signifies the post compaction, where the gradual disappearance of air void is usually shown. The only difference between the two is that a relatively small vertical loading width and radius (a tire width and its radius) are applied to rutting while a large width and radius (a roller width and its radius) are involved in compaction. That is, the loading mechanism is identical, but the geometry of loading device is different. Hence, the well known empirical rutting equation can be used to describe the deformation of compaction process as well, where rut depth (or compaction depth, h) is usually expressed in the term of wheel pass (or roller coverage, N) with two parameters (α and β) as

$$h = \alpha N^{\beta} \tag{4}$$

Insertion of Eqs. 4 into 3 gives the expression of compaction density in the term of number of roller coverages:

$$\rho - \rho_o = \frac{cm}{A}\alpha N^{\beta} \quad \text{or}$$

$$\mathrm{Ln}(\rho - \rho_o) = \mathrm{Ln}\left\{\frac{cm\alpha}{A}\right\} + \beta \mathrm{Ln}(N) \tag{5}$$

Equation 5 indicates that compaction density is related to number of roller coverages in the power form, and depends on the two parameters, α and β, just like rut depth in Eq. 4.

Geller (1977) compared density data of a vibratory roller to those of static ones. His data are plotted in Fig. 1 together with regression results by Eq. 5. The figure demonstrates well the linear relationship of the logarithmic plot, except the minor deviation of the two data points at the highest coverage. This may indicate appearance of the cooling effect, which will be covered later. Figure 1 manifests the better compaction performance of the vibratory roller over the static ones in the term of roller coverage.

As another example, Dellert (1977) studied the effect of roller speed on compaction density. His data are used to check Eq. 5 again. The validity is well displayed in Fig. 2. The low speed of a roller turns out to be better than the high one, as expected. However, cooling effect is absent in the speed analysis. If one accounts for the effect, one may choose the optimum speed instead of the slow one due to solidification.

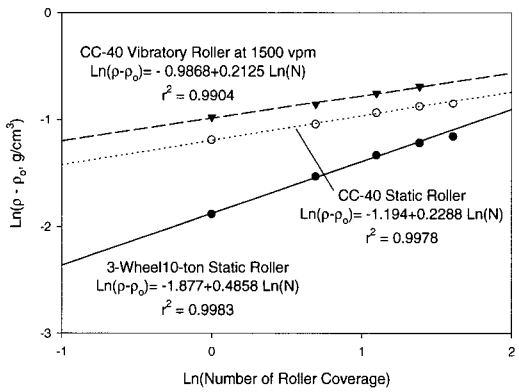

Fig. 1. Different roller effect on density for 8.255 cm paving lift.

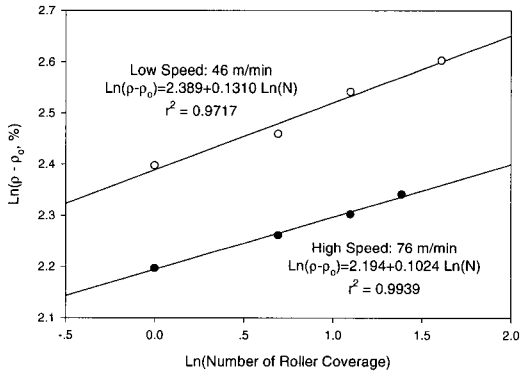

Fig. 2. Roller speed effect on density in the vibratory compaction.

Figures 1 and 2 clearly confirm the validity of Eq. 5 in describing temperature-independent compaction density in the term of roller coverage. The similar logarithmic linear relationship were extensively found in the work of Machet and Morel (1977). But they used density instead of the logarithmic density difference with respect to logarithmic number of coverages, and no theoretical justification were provided for their plots.

3. DEVELOPMENT OF THE DENSITY EQUATION

3.1 Total Applied Force

Dellert (1977) provided data for amplitude effect on density in the vibratory rolling. Figure 3 illustrates these data and curve-fitting results by Eq. 5. The excellent fittings are demonstrated again. The higher amplitude produces the larger density in the figure. Parameters, $cm\alpha/A$ and β, estimated from the regression in Fig. 3 are plotted in Fig. 4 in the term of the total applied force, representing amplitude. Here, the total applied force is defined as the sum of the static working weight of drum and the dynamic force per cycle developed by the vibrating mechanism. The parameter ($cm\alpha/A$) in Fig. 4(a) increases the total applied force (Ft) in the order of power, while the parameter β in Fig. 4(b) is linearly raised.

$$\frac{cm\alpha}{A} = k_1 \ F_t^{\ k_2} \qquad (6)$$

$$\beta = m_1 F_t + m_2 \qquad (7)$$

where k1, k2, m1 and m2 are constant parameters.

These two relationships are combined with Eq. 5 to express compaction density as a function of the total applied force (Ft):

$$\rho = \rho_o + k_1 \ F_t^{\ k_2} \ N^{(m_1 F_t + m_2)} \qquad (8)$$

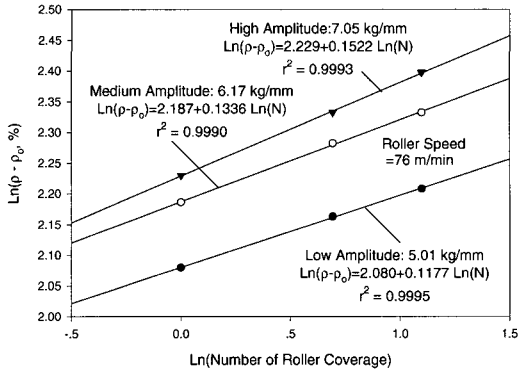

Fig. 3. Amplitude effect on density in vibratory rolling.

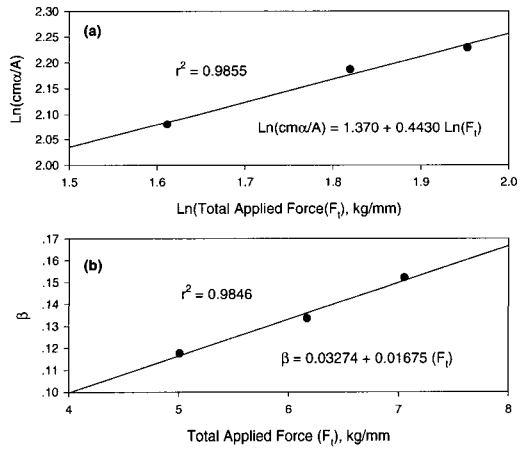

Fig. 4. Total applied force effect on density in vibratory rolling for (a) a parameter (cmα/A) and (b) a parameter (β).

3.2 Cooling Temperature Effect

Equation 5 starts to deviate from the logarithmic linear relationship when cooling effect comes into the compaction process. The low temperature increases mix zero shear viscosity (η_0), and thus compaction becomes difficult. Change of mix zero shear rate

viscosity (η_o) often affects the parameter a in Eq. 5. The viscosity expression of the a is given by Huh and Nam (1999) with constant parameters, d and k, as:

$$a = \frac{d}{\eta_o^{k\beta}} \tag{9}$$

Insertion of Eq. 9 into 5 yields

$$\rho - \rho_o = \frac{cm \cdot d}{A \ \eta_o^{k\beta}} N^{\beta} \tag{10}$$

Now, the relationship between mix viscosity and temperature is required to express the density difference of Eq. 10 as a function of temperature. This concept is successfully applied to the case of temperature change in rutting (Huh and Nam (1999)). According to them, Arrhenius temperature rule works well for the purpose: that is,

$$\eta_o = \eta_o^{\circ} \exp\left\{\frac{E_a}{R}\left(\frac{1}{T} - \frac{1}{T_o}\right)\right\} \tag{11}$$

Combination of Eqs. 10 and 11 produces

$$\rho - \rho_o = K \ \exp\left\{\frac{-M}{T}\right\} N^{\beta} \tag{12}$$

or

$$\mathrm{Ln}(\rho - \rho_o) = \mathrm{Ln}(K) - \frac{M}{T} + \beta \ \mathrm{Ln}(N) \tag{13}$$

where

$$K = \frac{cm \cdot d}{A \ \eta_o^{\circ k\beta}} \ \exp\left\{\frac{M}{T_o}\right\} \quad \text{and}$$

$$M = \frac{k\beta E_a}{R} \tag{14}$$

In the above equations, η_o°, T, T_o, E_a, and R represent the reference mix zero shear rate viscosity, the absolute Kelvin temperature, the reference absolute temperature, the activation energy for flow, and the universal gas constant, respectively.

Equation 12 (or 13) represents density difference as a function of mix viscosity, cooling temperature, and number of roller passes. Note that the temperature-dependent equation 13 is approximated to the temperature-independent Eq. 5, if the term, -M/T, is almost constant. This demonstrates that deviation from the linearity in logarithmic density difference versus logarithmic roller coverage is due to presence of the cooling term, -M/T in Eq. 13.

One additional equation, which specifies the cooling history as a function of roller pass, is needed in Eq. 12 (or 13). That is,

$$T = F(N) \tag{15}$$

By inserting Eq. 15 into 12 (or 13), the compaction density in the term of number of roller coverage is completed. Functional forms in Eq. 15 is turned out to be mostly linear,

$$T = A - BN \tag{16}$$

or sometimes quadratic.

$$T = A' + B'N - C' \ N^2 \tag{17}$$

where A' is the initial compaction temperature, and B' and C' are constants relating to the cooling rate.

Cechetini (1974) reported compaction density data in the term of roller coverage together with a history of temperature change. Equation 13 is used to fit the temperature-dependent density data and the result is displayed in Fig. 5(a). The temperature change in the term of roller coverage required in Eq. 13 is provided by Eq. 16 and is shown in Fig. 5(b). The linear region in Fig. 5(a) indicates negligible effect of temperature change in Eq. 13. Appearance of deviation from the linearity evidently starts from emergence of cooling term, -M/T. When number of coverages extends, the gradual increase of cooling effect permits the

density curve to reach the maximum, and then decrease further.

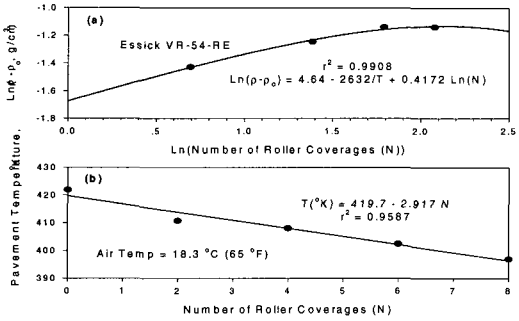

Fig. 5. Pavement temperature effect on density of asphalt mixes for (a) a regression result by Eq. 13 and (b) a linear cooling history.

However, decrease of density after the maximum point is not physically realistic. Beyond this point, no increase or decrease in compaction density should exist because the mix material is assumed to be solidified at the point.

Figure 6 clearly exhibits cooling effect on consolidation during compaction process. The dotted line indicates the linearity region, where cooling effect can be ignored. Deviation from the dotted line signifies appearance of the cooling effect, and it becomes more significant with increase of coverage.

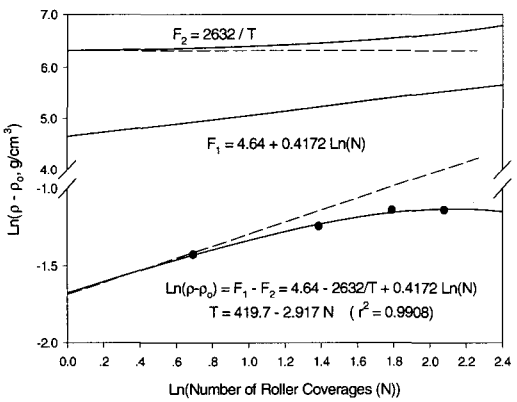

Fig. 6. Effect of cooling history on the logarithmic density.

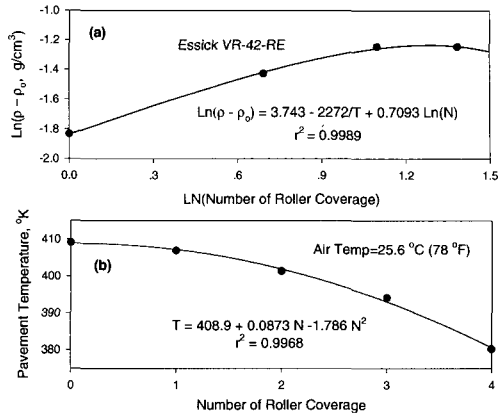

Fig. 7. Pavement temperature effect on density of asphalt mixes for (a) a regression result by Eq. 13 and (b) a quadratic cooling history.

Regression of density data using a quadratic coverage function (Eq. 17 and Fig. 7(b)) by Eq. 13 is illustrated in Fig. 7(a). The successful prediction is also observed. At a relatively higher coverage, the earlier onset of the maximum point is observed (due to the rapid cooling) compared to the linear coverage.

The maximum density (solidification density) is important in practice because all compaction activity should be completed before reaching the point. It is analytically obtained by differentiating Eq. 12 (or 13) with respect to number of coverages. For instance, by assuming a linear cooling history (Eq. 16), differentiation of Eq. 12 yields

$$\frac{d(\rho - \rho_o)}{dN} = \frac{d}{dN}\left[K \exp\left\{\frac{-\beta W}{A - BN}\right\} N^{\beta}\right] = 0 \tag{18}$$

which produces

$$N_m = \frac{(2A + W) - \sqrt{(4A + W)W}}{2B} \tag{19}$$

where $W = kE_a/R = M/\beta$.

Equation 19 states that the initial compaction temperature (A), the cooling rate

(B), and the thermal parameter (W) determine the maximum coverage. In the cooling history, the B is the cooling rate defined as a function of roller speed, distance and width of roadways to be covered, thickness of a lift layer, and air temperature. The k and E_a/R, which determine W, are binder properties relating to temperature change.

Behaviour of three parameters (W, A, and B) is demonstrated in Fig. 8(a), (b), and (c) for reference. The low value of parameter W yields the high maximum coverage in Fig. 8(a), but its magnitude depends on the thermal property of the asphalt mixture. The maximum coverage increases almost linearly with the initial compaction temperature A in Fig. 8(b). The higher value of A brings the lengthened maximum coverage, and leads to the better compaction. The smaller cooling rate B in Fig. 8(c) affects tremendously to raise the maximum coverage. Hence, among the three parameters, keeping the cooling rate to be small is most desirable in compaction. Especially, for the mix which is too hard to be compacted, choosing a high initial temperature and a low cooling rate is highly recommended.

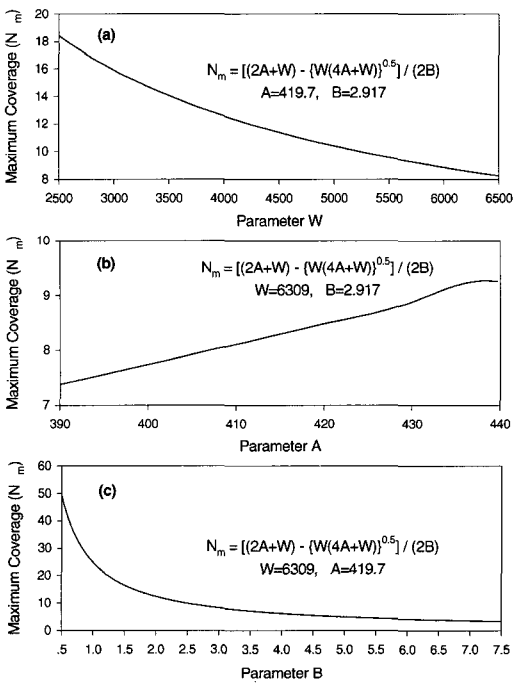

Fig. 8. Maximum coverage with respect to (a) W, (b) A, and (c) B in Figure 5.

The maximum coverage defined by Eq. 19 tends to be estimated a little higher than the experimentally observed one. Equation 19 evaluates Nm to be 8.5 instead of 6 observed in Fig. 5(a), while Nm is 5.4 instead of 4 observed in Fig. 7(a). Thus, the 97 percent of the maximum is recommended to be the right levelling-off value.

Once the maximum coverage (N_m) is known as shown by Eq. 19, the density at the maximum (ρ_m) is determined by inserting it into Eq. 12:

$$\rho_m = \rho_o + K \exp\left\{\frac{-M}{A - B N_m}\right\} \cdot N_m^{\beta} \quad (20)$$

Now, the total compaction achievable is obtained by the value of ($\rho_m - \rho_o$) in Eq. 20, and depends on K, M, A, B, β, and Nm.

Equations 12 and 20 are combined to give another expression of a compaction density function; that is,

$$\rho = \rho_o + (\rho_m - \rho_o) \exp \left\{\frac{-BM(N_m - N)}{(A - BN)(A - B N_m)}\right\} \left\{\frac{N}{N_m}\right\}^{\beta} \quad (21)$$

Equation 21 provides information about percent of the maximum density achievable with a given number of roller coverages. For instance, the roller coverage which requires 97 percent of the maximum density can be obtained as

$$\frac{\rho - \rho_o}{\rho_m - \rho_o} = \exp \left\{\frac{-BM(N_m - N)}{(A - BN)(A - B N_m)}\right\} \left\{\frac{N}{N_m}\right\}^{\beta} \geq 0.97 \quad (22)$$

The number of roller coverages corresponding to 97 percent of the maximum density is evaluated from Eq. 22. At this ninety-seven percent, the levelling-off coverage (N) becomes 6 for Fig. 5, while Fig. 7 produces a little over 4, which agree with observation.

3.3 Frequency Effect

When evaluating vibratory compactors, the three most important factors, which are frequency, amplitude, and weight of the compactor must be considered. Among them, the amplitude effect has been studied previously, and now the subject of the frequency is investigated. The required data are found from the work of Cechetini (1974). However, the data lacks the temperature history of compaction. For the analysis purpose, two arbitrary temperature variations are assigned.

Figure 9 shows the regression results of frequency data by Eq. 13 under the temperature change with a quadratic coverage. In a quadratic case, temperature cools slowly at low coverages, and then the rapid cooling takes place at the high end, as shown in Fig. 7(b). This trend is reflected well in Fig. 9, which displays a lengthy linear relationship at low coverages and then drastic decrease of density is shown after the maximum. Meanwhile, for the case of linear cooling history as shown in Fig. 10, the linearity region is shortened, and decrease of density after the maximum is not sharp compared to Fig. 9. This may suggest that degree of compaction can be controlled by choosing the right cooling history.

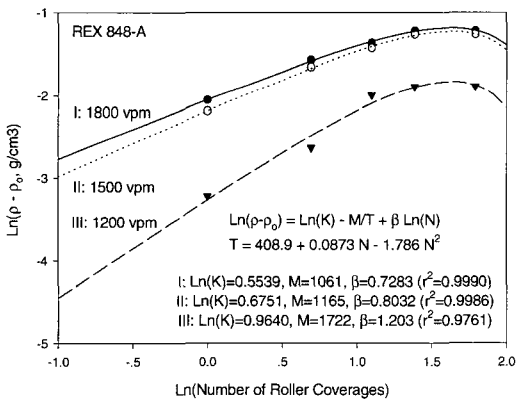

Fig. 9. Frequency effect on compaction density in vibratory rolling.

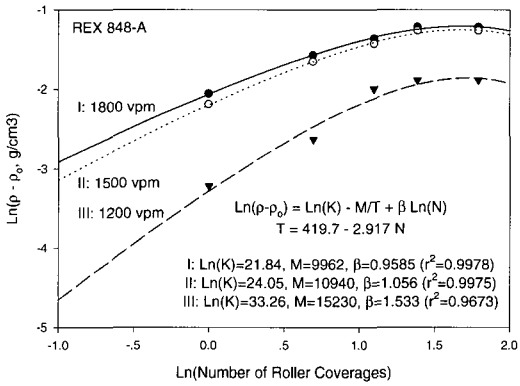

Fig. 10. Frequency effect on compaction density in vibratory rolling.

The estimated parameters of Eq. 13 (Ln(K), M, and β) shown in Figs. 9 and 10 are plotted with respect to frequency in Figs. 11 and 12. Those figures assert that the compaction frequency of vibratory rollers invokes a relaxation response on the density with a single relaxation time. That is,

$$R = R_o \exp\left\{\frac{t}{\lambda}\right\} = R_o \exp\left\{\frac{1}{\lambda}\frac{1}{f}\right\} \qquad (23)$$

where R, R_o, t, λ, and f are a parameter in Eq. 13, an initial parameter at t=0, a clock time, a relaxation time for compaction density, and a frequency, respectively. Note that a clock time corresponds to a reciprocal of a frequency, and the positive sign in the exponential term implies that the frequency response on magnitude of parameters is positive. Figs. 11

and 12 indicate that each cooling history owns its unique relaxation time.

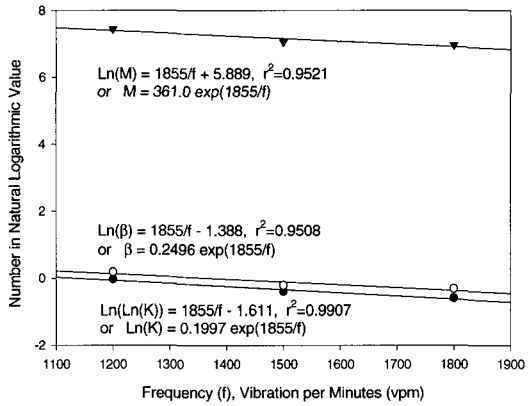

Fig. 11. Frequency effect on density parameters shown in Fig. 9.

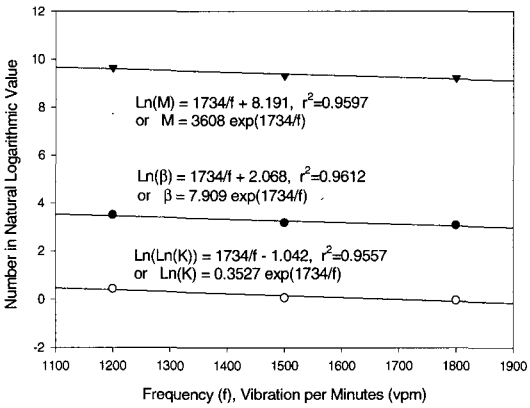

Fig. 12. Frequency effect on density parameters shown in Fig. 10.

3.4 A Full Compaction Density Equation

If the frequency effect, Eq. 23, is incorporated into Eq. 13, then the expression becomes

$$\mathrm{Ln}(\rho - \rho_o) = \left\{ \mathrm{Ln}(K) - \frac{M}{T} + \beta\ \mathrm{Ln}(N) \right\} \exp\left\{ \frac{1}{\lambda}\frac{1}{f} \right\} \quad (24)$$

Also, if the total applied force of Eq. 8, representing amplitude of vibratory rolling, is added into Eq. 24, it is written as

$$\mathrm{Ln}(\rho - \rho_o) = \left[\mathrm{Ln}\left\{ \frac{k_1\ F_t^{\,k_2}}{\eta_o^{\,k\beta}} \right\} - \frac{M}{T} + (m_1 F_t + m_2)\mathrm{Ln}(N) \right] \exp\left\{ \frac{1}{\lambda}\frac{1}{f} \right\} \quad (25)$$

Equation 25 explains compaction density as a function of mix zero shear rate viscosity, total applied force, cooling temperature, number of roller coverages, and frequency. Further verification of the equation may be needed with additional data in the future. Equation 25 can be for a quantitative analysis of the vibratory roller data. For the static rolling case, the static linear load and the infinite frequency must be used in the place of the total applied force (F_t) and the frequency (f) in Eq. 25.

4. DISCUSSIONS AND RESULTS

A main purpose of compaction study is to estimate the two important parameters: one is the number of roller coverages required to reach the levelling-off density and the other is the final density achieved by the particular compaction process. The former information is needed to finish a particular compaction job. Equation 22 demonstrates it as a function of mix viscosity, cooling temperature and roller coverage. Likewise, the latter informs a compaction degree achieved by a particular compaction job. Equation 20 exhibits one example.

If amplitude and frequency effects of vibratory rollers are included in Eq. 22, the number of roller coverages for the levelling-off density (NL) can be described as:

$$\frac{\rho - \rho_o}{\rho_m - \rho_o} = \exp\left\{\frac{-BM \exp(1/\lambda f)(N_m - N_L)}{(A - B N_L)(A - B N_m)}\right\} \cdot \left\{\frac{N_L}{N_m}\right\}^{(m_1 F_t + m_2)\exp(1/\lambda f)} \geq 0.97 \quad (26)$$

where

$$N_m = \frac{(2A + W) - \sqrt{(4A + W)W}}{2B} \quad (27)$$

Equation 26 tells that increase or decrease of a roller coverage require control of several variables like M ($=k\beta E_a/R$), λ, f, A, B, and W ($=kE_a/R$). Adjusting these variables, one can choose the desired roller coverage.

Likewise, the expression of the final density achieved (ρ_L) is obtained by referencing Eq. 20;

$$\rho_L = \rho_o + \left\{\frac{k_1 F_t^{k_2}}{\eta_o^{k\beta}}\right\}^{\exp(1/\lambda f)} \exp\left\{\frac{-M\exp(1/\lambda f)}{A - B N_L}\right\} \cdot N_L^{(m_1 F_t + m_2)\exp(1/\lambda f)} \quad (28)$$

Equation 28 suggests how each variable affects to increase or decrease the final density to be obtained. Control of these variables allows one to obtain the wanted final density. Thus, Eqs. 26 and 28 will serve to design the quality of a constructed asphalt pavement.

5. CONCLUSIONS

Density data with respect to number of roller coverages is a popular way of describing compaction process in pavement construction. The new theoretical equation to quantify the compaction density has been developed on the basis of the empirical rutting equation. The equation suggests the logarithmic linear relationship between density difference and roller coverage, and turns out to work well under a constant temperature. In addition, the effects of cooling temperature, amplitude, and frequency are also investigated. The results are incorporated into a general density equation suggested. Further validation may be demanded in the future.

In conclusion, a new tool for a systematic study of compaction is supplied in this study. The tool may help to predict and control compaction process more accurately such that pavement performance improve significantly.

REFERENCES

1. Cechetini, J.A. (1974), Vibratory Compaction of Asphalt Concrete Pavements, J. Assoc. of Asphalt Paving Technol., 43, pp. 384-416.
2. Dellert, R.B. (1977), Vibratory Compaction of Thin Lift Asphalt Resurfacing, J. Assoc. of Asphalt Paving Technol., 46, pp. 287-293.
3. Geller, M. (1977), Summarizing the Development of Vibratory Roller Applications for Compacting Bituminous Mixes in the USA, J. Assoc. of Asphalt Paving Technol., 46, pp. 272-279.
4. Huh, J.D. and Nam, Y.K. (1999), A New Theory for Temperature Dependence of Rutting, KSCE J. of Civil Engineering, Vol. 3, No. 2, pp. 159-169.
5. Linden, F. and Heide, J.V.D. (1977), Some Aspects of the Compaction of Asphalt Mixes and Its Influence on Mix Properties, J. Assoc. of Asphalt Paving Technol., 56, pp. 408-426.
6. Machet, J.-M. (1977), Vibratory Compaction of Bituminous Mixes in France, J. Assoc. of Asphalt Paving Technol., 46, pp. 326-340.